Convergence of Solutions of Shape Design Problems For Fluid Flow at Long Time Horizons ⋆

John Sebastian H. Simon *

* *Division of Mathematical and Physical Sciences, Graduate School of Natural Science and Technology, Kanazawa University, Kanazawa 920-1192, Japan (e-mail: john.simon@stu.kanazawa-u.ac.jp, jhsimon1729@gmail.com).*

1. INTRODUCTION

Let $\mathcal{D} \subset \mathbb{R}^2$ be a non-empty open bounded connected domain, $\omega \subsetneq \mathcal{D}$, and consider the following set of admissible domains

$$\mathcal{O}_\omega = \{\Omega \subset \mathcal{U} : \Omega \supset \omega,\ \Omega \text{ is open, bounded, connected, and at least of class } C^{0,1}\}.$$

Let $\boldsymbol{f} \in L^2(\mathcal{D};\mathbb{R}^2)$ be a stationary fluid source function, which can be interpreted as the force that steers the fluid at a constant pace—an example of this is a fluid pump and fluid outlet that act on the fluid at the same rate— and $\Omega \in \mathcal{O}_\omega$. The time-dependent Navier–Stokes equations on the interval $(0,T)$ is given by

$$\begin{cases} \partial_t \boldsymbol{u} - \nu\Delta\boldsymbol{u} + \gamma(\boldsymbol{u}\cdot\nabla)\boldsymbol{u} + \nabla p = \boldsymbol{f} & \text{in } \Omega\times(0,T), \\ \nabla\cdot\boldsymbol{u} = 0 & \text{in } \Omega\times(0,T), \\ \boldsymbol{u} = 0 & \text{in } \partial\Omega\times(0,T), \\ \boldsymbol{u} = \boldsymbol{u}_0 & \text{in } \Omega\times\{0\}, \end{cases} \tag{1}$$

where $\boldsymbol{u}$ and p correspond to the dynamic fluid velocity and pressure, respectively, and $\boldsymbol{u}_0 \in L^2(\mathcal{U};\mathbb{R}^2)$ is the initial velocity that satisfies $\nabla\cdot\boldsymbol{u}_0 = 0$ in Ω. The parameter $\nu > 0$ denotes the fluid viscosity. On the other hand, we call $\gamma \geq 0$ the *convection parameter*. We also look at the stationary Navier–Stokes equations

$$\begin{cases} -\nu\Delta\boldsymbol{v} + \gamma(\boldsymbol{v}\cdot\nabla)\boldsymbol{v} + \nabla q = \boldsymbol{f} & \text{in } \Omega, \\ \nabla\cdot\boldsymbol{v} = 0 & \text{in } \Omega, \\ \boldsymbol{v} = 0 & \text{in } \partial\Omega, \end{cases} \tag{2}$$

where $\boldsymbol{v}$ and q are the equilibrium fluid velocity and pressure, respectively.

On both equations, if $\gamma = 1$ we reduce to the usual Navier–Stokes equations, while $\gamma = 0$ gives us the Stokes equations.

We focus on the analysis of two shape optimization problems governed by equations (1) and (2). In particular, given a static desired velocity $\boldsymbol{u}_D \in L^2(\omega;\mathbb{R}^2)$, we consider the time-average problem

$$\left.\begin{array}{c} \min\limits_{\Omega\in\mathcal{O}_\omega} J_T(\Omega) := \dfrac{\nu}{T}\displaystyle\int_0^T \|\boldsymbol{u}(t) - \boldsymbol{u}_D\|^2_{L^2(\omega;\mathbb{R}^{2\times 2})}\,\mathrm{d}t \\ \text{subject to (1),} \end{array}\right\} \tag{3}$$

and the stationary shape design problem

$$\left.\begin{array}{c} \min\limits_{\Omega\in\mathcal{O}_\omega} J_s(\Omega) := \nu\|\boldsymbol{v} - \boldsymbol{u}_D\|^2_{L^2(\omega;\mathbb{R}^2)} \\ \text{subject to (2).} \end{array}\right\} \tag{4}$$

We denote the solutions of (3) and (4) by Ω_T and Ω_s. Our goal is to show that

$$|J_T^* - J_s^*| \leq c\left(\frac{1}{T} + \frac{1}{\sqrt{T}} + \frac{\gamma}{2^{1/2}}\right) \tag{5}$$

where $J_T^* := J_T(\Omega_T)$, $J_s^* := J_s(\Omega_s)$, and the constant $c := c(\boldsymbol{u}_0, \boldsymbol{u}_D, \boldsymbol{f}, 1/\nu, \mathcal{U}) > 0$ is independent of T.

Inequality (5) attempts to answer the contention that solutions to dynamic fluid shape design problems are close to the solution of the equilibrium problem. This assumption is one of the reasons why majority of shape optimization problems involving fluid deals with the stationary state equations rather than the time-dependent case.

Remark 1. Note that when $\gamma = 0$, both systems (1) and (2) can be realized as parabolic and elliptic problems, respectively, and inequality (5) reduces to the estimate of Trelat et al. (2018).

Our result is summarized in the following theorem.

Theorem 2. Suppose that $\boldsymbol{f} \in L^2(\mathcal{U};\mathbb{R}^2)$, $\boldsymbol{u}_0 \in H(\Omega) \cap L^2(\mathcal{U};\mathbb{R}^2)$, and $\boldsymbol{u}_D \in L^2(\omega;\mathbb{R}^2)$. If $J_T^* := J_T(\Omega_T)$ and $J_s^* := J_s(\Omega_s)$, where Ω_T and Ω_s are the solutions of (3) and (4), respectively; then there exists $c > 0$, independent of T, such that (5) holds.

As a consequence, we obtain a sense of convergence of solutions of (3) to a solution of (4). We formalize this result below.

Corollary 3. Suppose that the assumptions in Theorem 2 hold. Then there exists $\Omega^* \in \mathcal{O}_\omega$, such that $\Omega_T \xrightarrow{\chi} \Omega^*$ as $T \to \infty$, and that $|J_s^* - J_s(\Omega^*)| \leq 2^{1/2}c\gamma$, where $c > 0$ is the same constant as in Theorem 2. Here, the symbol $\xrightarrow{\chi}$ denotes the domain convergence with respect the the indicator functions in L^∞-topology.

2. NUMERICAL REALIZATION

To solve the problem numerically, we rely on a gradient descent method induced by the identity perturbation operator. For more details, we refer to Delfour and Zolesio

⋆ This work is supported by the Japanese Government Ministry of Education, Culture, Sports, Science and Technology (MEXT) Scholarship.

(2011). We compute the shape derivative of the objective functions in the sense of Hadamard's, i.e., the shape derivative of a given objective function $\mathcal{J} : \mathcal{O}_\omega \to \mathbb{R}$ in the direction of $\theta \in \Theta$ is denoted and defined as $d\mathcal{J}(\Omega)\theta = \lim_{\tau \searrow 0} \frac{\mathcal{J}(\Omega_\tau) - \mathcal{J}(\Omega)}{\tau}$.

The shape derivative of J_T and J_s have already been computed (see Kasumba and Kunisch (2012), and Mohammadi and Pironneau (2010) among others), hence we skip such step in this exposition. Nevertheless, such derivatives are given below

$$dJ_T(\Omega)\theta = \frac{\nu}{T}\int_0^T \left[\int_{\partial\Omega} (\partial_{\boldsymbol{n}}\boldsymbol{u}(t)\cdot\partial_{\boldsymbol{n}}\boldsymbol{w}(t))\theta\cdot\boldsymbol{n}\,\mathrm{d}\sigma + \int_\Omega \nabla\cdot(\chi_\omega|\boldsymbol{u}(t)-\boldsymbol{u}_D|^2\theta)\,\mathrm{d}x\right]\mathrm{d}t,$$

$$dJ_s(\Omega)\theta = \nu\left[\int_{\partial\Omega} (\partial_{\boldsymbol{n}}\boldsymbol{v}\cdot\partial_{\boldsymbol{n}}\boldsymbol{z})\theta\cdot\boldsymbol{n}\,\mathrm{d}\sigma + \int_\Omega \nabla\cdot(\chi_\omega|\boldsymbol{v}-\boldsymbol{u}_D|^2\theta)\,\mathrm{d}x\right],$$

where $\boldsymbol{w} \in L^\infty(I; H(\Omega)) \cap L^2(I; V(\Omega))$ is the time dependent adjoint variable that satisfies the variational problem

$$\begin{aligned}&{}_{V^*(\Omega)}\langle -\partial_t\boldsymbol{w}(t), \boldsymbol{\varphi}\rangle_{V(\Omega)} + \nu(\nabla\boldsymbol{w}(t), \nabla\boldsymbol{\varphi})_\Omega\\ &+ \gamma[((\boldsymbol{\varphi}\cdot\nabla)\boldsymbol{u}(t), \boldsymbol{w}(t))_\Omega - ((\boldsymbol{u}(t)\cdot\nabla)\boldsymbol{w}(t), \boldsymbol{\varphi})_\Omega]\\ &= 2(\boldsymbol{u}(t)-\boldsymbol{u}_D, \boldsymbol{\varphi})_\omega \quad \forall\boldsymbol{\varphi}\in V(\Omega),\end{aligned}$$

and the transversality condition $\boldsymbol{w}(T) = 0$, while $\boldsymbol{z} \in V(\Omega)$ solves the equation

$$\begin{aligned}&\nu(\nabla\boldsymbol{z}, \nabla\boldsymbol{\varphi})_\Omega + \gamma[((\boldsymbol{\varphi}\cdot\nabla)\boldsymbol{v}, \boldsymbol{z})_\Omega - ((\boldsymbol{v}\cdot\nabla)\boldsymbol{z}, \boldsymbol{\varphi})_\Omega]\\ &= 2(\boldsymbol{v}-\boldsymbol{u}_D, \boldsymbol{\varphi})_\omega \quad \forall\boldsymbol{\varphi}\in V(\Omega).\end{aligned}$$

Note that both derivatives can be expressed with the Zolesio-Hadamard structure, i.e., we can write

$$d\mathcal{J}(\Omega)\theta = \int_{\partial\Omega} \nabla J\boldsymbol{n}\cdot\theta\,\mathrm{d}\sigma,$$

where ∇J is called the shape gradient.These shape gradients will be the basis of our descent directions, i.e., by choosing $\theta = -\nabla J\boldsymbol{n}$ in $\partial\Omega$ we are assured that

$$d\mathcal{J}(\Omega)\theta = -\|\theta\|^2_{L^2(\partial\Omega;\mathbb{R}^2)} < 0.$$

Numerically though, such choice of descent direction may cause oscillations on the perturbed domains. Because of that, we shall resort to a traction method that intends to extend the choice of θ to the whole domain, say for example by a Robin boundary problem, see Azegami and Takeuchi (2006).

The variational equations are solved using Galerkin finite element methods. The stationary Navier–Stokes equations is solved using Newton's method, the dynamic Navier–Stokes equations and the time-dependent adjoint equation are solved using a Lagrange–Galerkin method based on characteristics, and the stationary adjoint equation is solved by the usual Galerkin method.

2.1 Numerical Implementation

For simplicity, we choose $\boldsymbol{f} = \frac{1}{10}(y^3, -x^3)$, the desired function is the solution of the Stokes equations with $\nu = 1/5$ in a domain enclosed in a circle that satisfies $x^2 + y^2 = 4$, and the domain $\omega \subset \mathbb{R}^2$ is the set $\{(x,y)\mathbb{R}^2 : x^2 + y^2 \leq 1\}$. The shape optimization problems are then solved with parameter values $\nu = \gamma = 1$, and with the initial velocity $\boldsymbol{u} = 0$.

To illustrate the convergence of the solutions of the time-dependent problems, we have Figure 1. Figure 1(A) shows that the boundary of the solutions $\partial\Omega_{T,h}$ becomes closer to the boundary $\Omega_{s,h}$ as the terminal time T gets bigger. Figure 1(B) shows the log-log plot of the gap $|J_T - J_s|$ versus the terminal time T. In the same figure, we plotted the plots of $\mathcal{O}(T^{-1})$ and $\mathcal{O}(T^{-1/2})$. Coincidental with the theoretical result, for lower values of T the order of convergence nearly follows $\mathcal{O}(T^{-1/2})$, while we observe a convergence that is similar with $\mathcal{O}(T^{-1})$ for higher values of T.

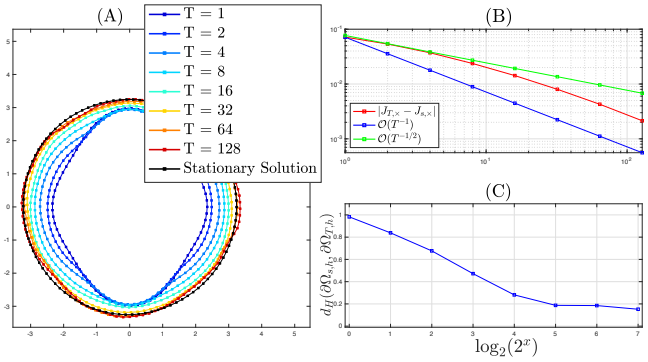

Fig. 1. Illustration of how the boundary of the shape solution of the time-dependent problem (3) converges to the boundary of the solution of the equilibrium problem (4) as T gets larger (A); log-log plots of $|J_{T,\times} - J_{s,\times}|$, $\mathcal{O}(T^{-1})$, and $\mathcal{O}(T^{-1/2})$(B); trend of the Hausdorff distance between the solutions of (3) and (4) (C).

Lastly, we quantified the convergence of the boundaries by virtue of the Hausdorff distance. We observe in Figure 1(C) that the Hausdorff distance indeed gets smaller as the value of x, which is such that $T = 2^x$, increases.

REFERENCES

Azegami, H. and Takeuchi, K. (2006). A smoothing method for shape optimization: Traction method using the Robin condition. *International Journal of Computational Methods*, 03(01), 21–33. doi: 10.1142/S0219876206000709.

Delfour, M. and Zolesio, J.P. (2011). *Shapes and Geometries: Metrics, Analysis, Differential Calculus, and Optimization*. Society for Industrial and Applied Mathematics, 2 edition.

Kasumba, H. and Kunisch, K. (2012). Vortex control in channel flows using translational invariant cost functionals. *Computational Optimization and Applications*, 52(3), 691–717. doi:10.1007/s10589-011-9434-y.

Mohammadi, B. and Pironneau, O. (2010). *Applied Shape Optimization for Fluids*. Numerical Mathematics and Scientific Computation. Oxford University Press.

Trelat, E., Zhang, C., and Zuazua, E. (2018). Optimal shape design for 2d heat equations in large time. *Inverse Problems in Science and Engineering*, 3(1), 255–269.